AIAA SPACE 2012 Conference & Exposition
11 - 13 September 2012, Pasadena, California

AIAA 2012-5199

Analyses of Cryogenic Propellant Tank Pressurization based upon Ground Experiments

C. Ludwig*
DLR, German Aerospace Center, Institute of Space Systems, 28359 Bremen, Germany
M. E. Dreyer†
ZARM, University of Bremen, 28359 Bremen, Germany

The pressurization system of cryogenic propellant rockets requires on-board pressurant gas. The objective of this study was to analyze the influence of the pressurant gas temperature on the required pressurant gas mass in terms of lowering the launcher mass. First, ground experiments were performed in order to investigate the pressurization process with regard to the influence of the pressurant gas inlet temperature. Second, a system study for the cryogenic upper stage of a small Two Stage to Orbit (TSTO) launch vehicle was performed with focus on the influence of the pressurant gas temperature on the propellant management system mass. One important experimental result is that for evaporated propellant as pressurant gas, the maximum applicable gas temperature is best for reducing the needed pressurant gas, but on condition that all pressurization lines are chilled down. Moreover, the use of helium is very advantageous with regard to lowering the pressurant gas mass. Also significant is that an immediate pressure drop occurred after the pressurization end. The conclusion drawn from the system analysis is that an increased evaporated propellant and helium pressurant gas temperature resulted in a decrease of the total propellant management system mass, despite the application of external helium vessels.

Nomenclature

D_t	Thermal diffusion coefficient, m^2/s
H	Fluid height
I_{sp}	Specific impulse, s
p	Pressure, kPa
Q_w	Heat of dewar wall, W
T	Temperature, K
t	Time, s
$t_{p,0}$	Start of pressurization, s
$t_{p,f}$	End of pressurization, s
$t_{p,f} + T$	Specific time after pressurization end, s
z	Height coordinate, m

Subscripts

f	Final
l	Liquid
p	Pressurization
pg	Pressurant gas
sat	Saturation
v	Vapor
vac	Vacuum

*Aerospace Engineer, Space Launcher Systems Analysis (SART), carina.ludwig@dlr.de, Member AIAA
†Head of Department Fluid Dynamics and Multiphase Flow

I. Introduction

In the recent decades, the aerospace industry has put great effort into increasing the payload mass of launchers. Therefore, cryogenic upper stages came back into focus, since they offer an increased payload capacity due to the very high specific impulse of their engines. For this upper stage concept, weight savings are enormously important, since the first stage has to carry the upper stage during ascent. Ring[1] stated, that for ICBM (intercontinental ballistic missiles) two-stages vehicles the second-stage weight is approximately ten times as important as the weight of the first-stage. Consequently, high effort should be made to design minimum-weight cryogenic upper stages for launchers.

One important subsystem of the propellant management system of cryogenic stages is the pressurization system. It is part of the feed system and controls the gas pressure in the ullage of the propellant tanks in order to maintain the preselected tank pressure history. Due to the very low temperatures of cryogenic fluids, complex fluid-mechanical and thermodynamic processes occur during pressurization inside the propellant tank, which are not yet fully understood. Since tank pressurization requires the use of on-board fluids, optimization of the pressurization process is essential in order to lower the stage's mass and therewith to increase the payload mass.

Experimental research in these fields had been pursued in the USA primarily during the Apollo missions. In 1966, Nein et al.[2] presented experimental results of pressurization gas requirements of cryogenic liquids. The experimental work was conducted on five different LOX (liquid oxygen) tank configurations. The major results were that no significant radial ullage temperature gradient occured and that the heat transfer between pressurant and tank walls could differ significantly from free convection, depending on tank and diffuser design. He also stated that the strongest influence on the pressurant mass was the pressurant gas inlet temperature. Further influence came from the tank radius as well as the pressurant gas distributor flow area.

Stochl et al.[3–6] performed experimental investigations on the tank pressurization and expulsion of spherical LH2 (liquid hydrogen) tanks with two different diameters of 1.52 m and 3.96 m. As pressurant gases, GH2 (gaseous hydrogen) as well as GHe (gaseous helium) was used. One major outcome of these experiments was that the pressurant gas inlet temperature had the strongest effect on pressurant gas requirements and that an increased pressurant gas temperature decreased the pressurant required for constant ramp rates.

Based on these results, other experiments on the pressurization of cryogenic liquids have been performed. In 1991, van Dresar and Stochl[7] presented requirements for a low-gravity experiment for the pressurization and expulsion of a cryogenic supply tank. They predicated that the amount of required pressurant gas depends, besides the volume of the liquid displaced, upon the heat transfer into the liquid and the tank wall as well upon the amount of mass condensed and evaporated. In 1993, van Dresar and Stochl[8] introduced experimental results of pressurization and expulsion of LH2 in normal gravity. The major result was that pressurant consumption increased significantly with increased operational time. Additionally, they stated that for the tank ullage, the gas-to-wall heat transfer was the dominant mode of energy exchange with more than 50% of pressurant energy being lost.

In 2002, Himeno[9] showed the importance of a good design of the pressurization system by presenting data collected at the maiden flight of the HII-A launcher's cryogenic upper stage. The dynamic motion of LH2 in the upper stage tank was observed with a camera. One result was that under low-gravity condition, the injected GHe pressurant gas penetrated deeply into the liquid propellant. Based on that occurrence, the diffuser design was changed.

The presented experiments enormously advanced the development of launchers and brought some general understanding of the requirements of a pressurization system. But these studies are lacking a specific analysis of the influence of the pressurant gas inlet temperature on initial active-pressurization of cryogenic propellants with regard to effects on the whole launcher stage.

On that account, the objective of this paper was to answer the following questions: Which pressurant gas inlet temperature requires least pressurant gas mass? How much does this influence the mass of the whole propellant management system?

II. Experiments

In order to further understand the thermodynamics and fluid-mechanics during the initial active-pressurization process of cryogenic fluids, ground experiments were performed focusing on the influence of the pressurant gas inlet temperature on the active-pressurization process. For these experiments, liquid nitrogen (LN2) was used as a cryogenic propellant substitute, which was actively pressurized under normal gravity conditions up to different final tank pressures. As pressurant gases, gaseous nitrogen (GN2) and gaseous helium (GHe) were used with different inlet temperatures. The following section describes the experimental set-up and presents the main results.

A. Experimental Set-up and Procedures

The test facility used for this study is schematically depicted in figure 1. It consists of a storage bottle for the pressurant gas, a mass flow controller, which ensures a constant pressurant gas mass flow, a heat exchanger, which can influence the pressurant gas temperature, and the high pressure dewar, partly filled with liquid nitrogen, in which the active-pressurization takes place and where the pressure is measured. Valves are used to control the flow. A more detailed view of the high pressure dewar is depicted in figure 2. It is a

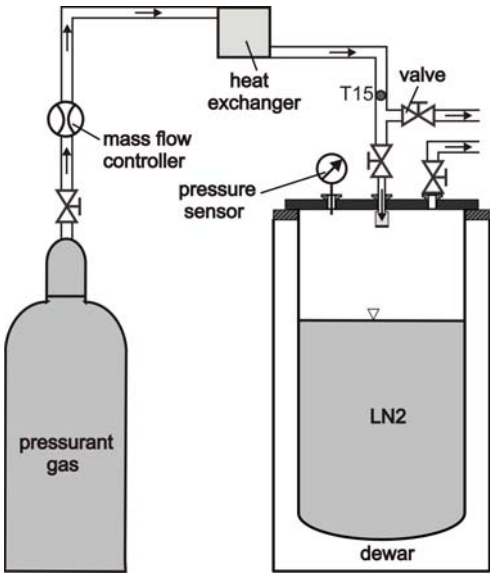

Figure 1. Drawing of the experimental set-up

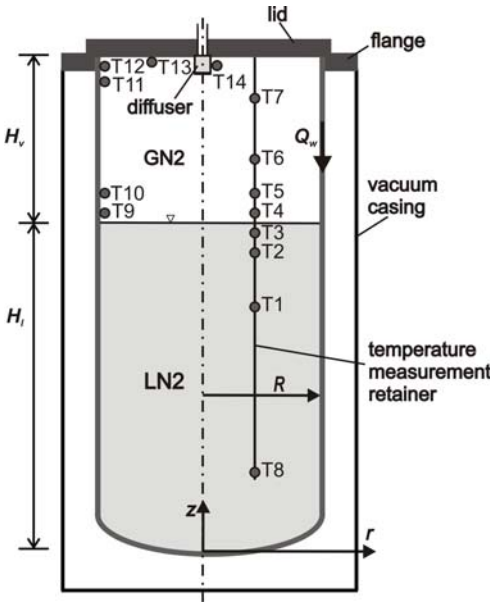

Figure 2. Dewar with locations of temperature sensors

cylindrical cryostat with a round shaped bottom placed in a vacuum casing. The dewar has an internal volume of 43 liter and is filled by two thirds with LN2. The liquid-vapor interface is at $z = H_l = 0.445$ m, the height of the tank ullage is $H_v = 0.205$ m, and the dewar radius is $R = 0.148$ m. The entering pressurant gas is distributed by the diffuser, which is a sintered filter. The diffuser is sealed at the bottom so that the pressurant can only leave the filter radially, in order to protect the liquid surface from a direct jet.
The temperature inside the dewar is logged at 14 pre-defined positions with silicium diodes. The positions of the temperature sensors are marked in figure 2 with black dots. The temperature sensors T1 to T8 are arranged on a retainer in order to measure the temperature of the fluids. The sensors T1, T2, T3 and T8 are placed in the liquid nitrogen, sensors T4 to T7 in the tank ullage. The free surface is situated in the middle between the sensors T3 and T4. The sensors T9 to T12 measure the dewar wall temperatures at different heights in the tank ullage and sensor T13 determines the temperature at the inner side of the lid. The temperature sensor T14 is placed next to the diffuser in order to log the temperature of the injected pressurant gas.

In order to guarantee the same initial stratification conditions for each experiment, the dewar was overfilled with LN2 at a pre-set time, several hours before the experiment start, and the tank outlet valve (comp. figure 1) was partly opened so that the evaporated nitrogen could leave the dewar. When the liquid surface reached the pre-defined position in the middle between the temperature sensors T3 and T4, the actual active-pressurization experiment was started. Then the bleed next to T15 was opened and the feed lines from the pressurant gas storage bottle to the branching were chilled down. In the next step, the dewar outlet valve was closed and the inlet valve opened. Now, the dewar was pressurized as pressurant gas was fed into the dewar. When the final tank pressure was reached, the inflow was stopped by closing the tank inlet valve of the dewar, so no mass could enter or leave the tank. Inside the dewar, relaxation took place. After a pre-set time, the dewar outlet valve was opened again and the experiment was completed. During the whole experiment, the tank pressure and the temperatures were logged.
For this study, either GN2 or GHe was used as pressurant gas. For the GN2 experiments, four different pressurant gas temperatures T_{pg} were chosen, measured at T15 (comp. figure 1), to reach three different final tank pressures p_f (see table 1) and for the GHe pressurization two pressurant gas temperatures with two final tank pressures were selected (see table 2).

Table 1. Experimental matrix of GN2 pressurization

p_f [kPa]	T_{pg} [K]			
200	144	263	294	352
300	144	263	294	352
400	144	263	294	352

Table 2. Experimental matrix of GHe pressurization

p_f [kPa]	T_{pg} [K]	
200	263	352
400	263	352

B. Experimental Results

Hereafter, the main results of the performed experiments are presented: the pressure and temperature evolution, the history of fluid stratification, and the required pressurant gas mass.

1. Pressure and Temperature Evolution

The consideration of the initial conditions inside the dewar prior to the pressurization is essential for understanding the behavior during and after pressurization. At initial conditions, the tank ullage is only filled with evaporated nitrogen, representing a two phase system with a single fluid. The average initial tank pressure is 106 kPa. For the presented experiments, the lid always had an outer temperature of 280 K, and due to its construction a constant inner lid temperature of 278 K. The temperature of the free surface is always considered to be the saturation temperature of the current tank pressure.[10]
Figure 3 depicts pressure and temperature evolution of the pressurization experiment GN2_300kPa@352K, wherefore the GN2 pressurant gas inlet temperature is 352 K at T15 and the final tank pressure is 300 kPa. The tank pressure (figure 3 (a)) increases almost linearly up to the final pressure and then decreases rapidly as no more pressurant gas is injected. Due to the fact that the dewar is kept closed, relaxation takes place and the pressure curve asymptotically decreases to 250 kPa. Because of the fast pressurization process, the condensation during the pressurization is not finished at pressurization end and GN2 also condenses also afterwards and reduces the tank pressure. The pressure drop ends at that time when the amount of evaporated fluid at the wall equals the amount of condensed fluid at the free surface.
For the liquid temperature (figure 3 (b)), only the two uppermost temperature sensors detected a change in temperature over the considered time frame. One main reason is that condensation takes place during the pressurization process at the free surface and the latent heat which is released increases the temperature only in the uppermost liquid layer. Another reason is that heat is conducted from the comparatively warm flange of the cryostat into the dewar wall (see Q_w in figure 2). The flange is an undesired thermal connection between the vacuum casing with ambient temperature and the inner dewar wall. The majority of this heat was yielded into the liquid at the free surface, also increasing the thermal gradient in the uppermost liquid layer. The third, but least heat flow is heat conduction from the ullage over the free surface. The total heat, introduced in the uppermost liquid layer is slowly conducted downwards and increased the thermal boundary layer, as can be seen by comparing T3 and T2 in figure 3 (b).

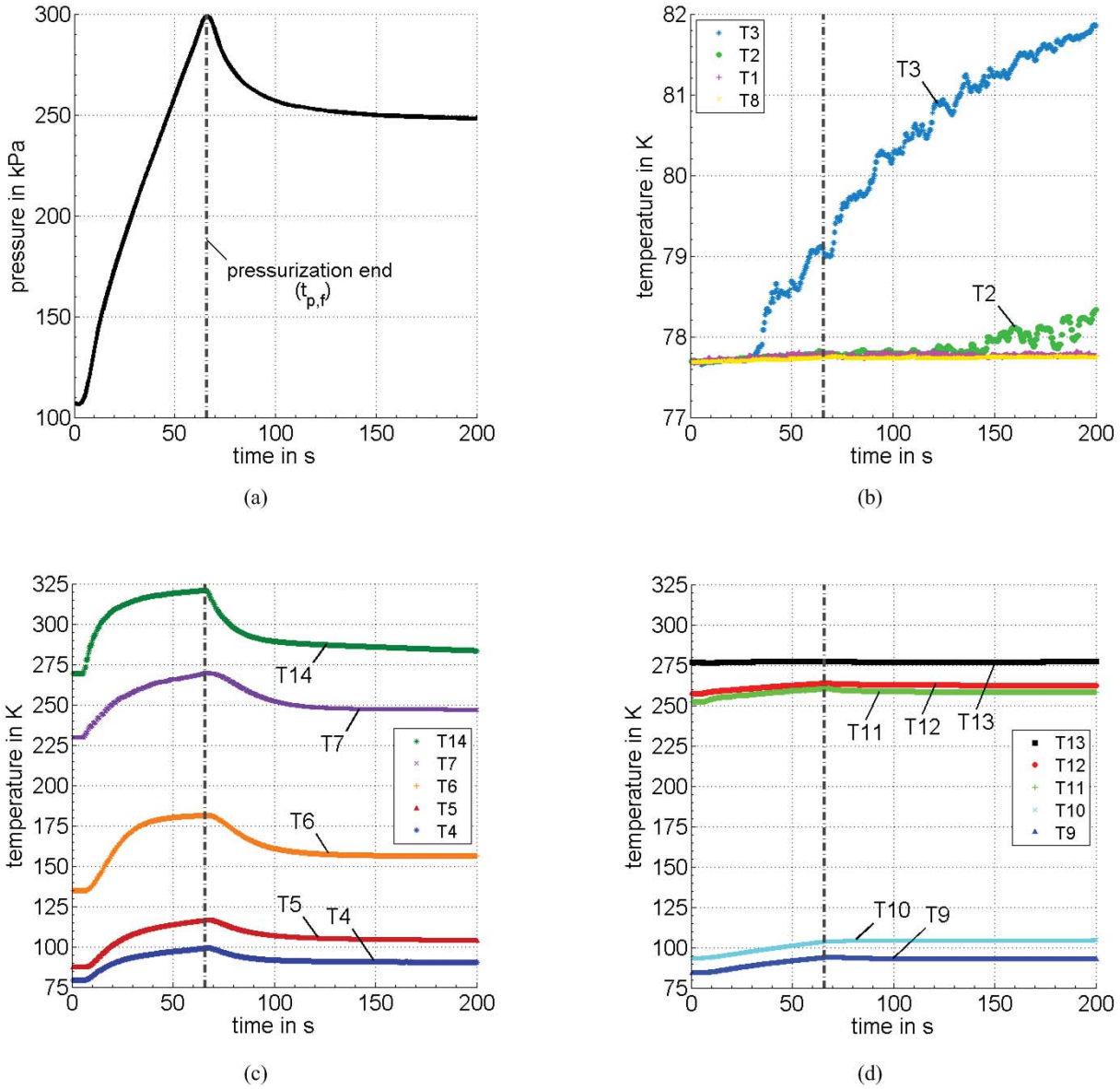

Figure 3. (a) Tank pressure, (b) liquid temperatures, (c) vapor temperatures, (d) wall and lid temperatures during pressurization and relaxation of the GN2_300kPa@352K experiment. Pressurization starts at $t_{p,0}$ (t= 5 s) and ends at $t_{p,f}$ (t= 66 s).

In the vapor temperature evolution (figure 3 (c)), the influence of the hot pressurant gas on the stratification during the pressurization process can be seen. The hot pressurant gas is increasing the temperature of the vapor with decreasing impact from the lid downwards. This indicates that there is moderate forced convection in the vapor phase, initiated by the diffuser flow. After the end of the pressurization, the temperatures reduces analogously to the pressure. The pressurant gas temperature at sensor T14 is not constant over time since the connecting pipe between the tank inlet valve and the diffuser has to adapt to the gas temperature as it could not be chilled down before the pressurization.
The wall temperatures (figure 3 (d)) are also affected by the pressurization process, but much less than the vapor temperatures due to the slow reaction of the wall material. It can be seen that the lid temperature is not changing over time.
The presented pressure and temperature evolutions are also similar for the GHe pressurization experiments.

2. Evolution of Fluid Stratification

The active-pressurization process has a big influence on the thermal stratification in the liquid and vapor phase of the dewar. Therefore, the evolution of the stratification in the fluids is analyzed. The moment before pressurization starts ($t_{p,0}$ at t= 5 s), the end of pressurization ($t_{p,f}$ at t= 66 s) and after relaxation ($t_{p,f} + T$ at t= 200 s) are defined as the characteristic times. As an example the same GN2 pressurization experiment as previously shown in figure 3 is analyzed.

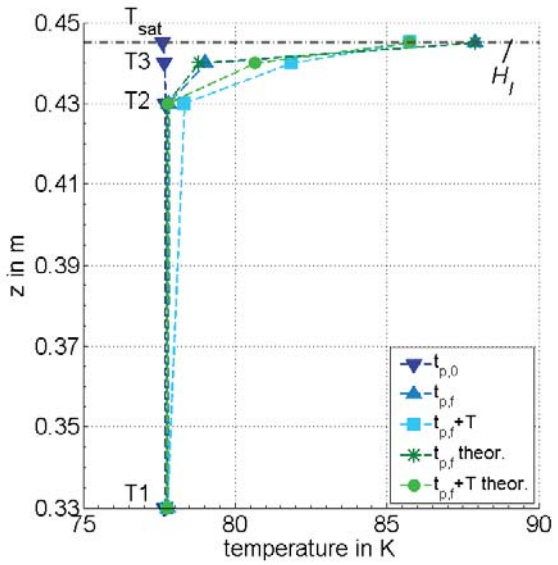

Figure 4. Experimental liquid temperature profiles before pressure ramping ($t_{p,0}$), at pressurization end ($t_{p,f}$) and after relaxation ($t_{p,f} + T$) of the GN2_300kPa@352K experiment. Theoretical temperature profile with formula 1. Dashed lines are only for better visualization.

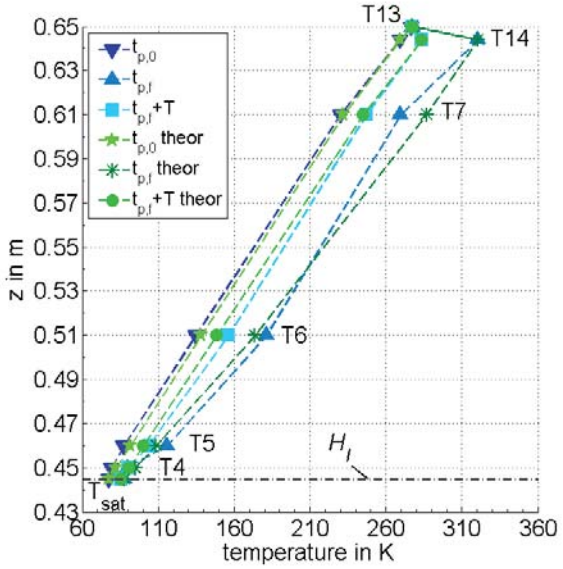

Figure 5. Experimental vapor temperature profiles before pressure ramping ($t_{p,0}$), at pressurization end ($t_{p,f}$) and after relaxation ($t_{p,f} + T$) of the GN2_300kPa@352K experiment. Theoretical temperature profile with formula 2 at $t_{p,0}$ and $t_{p,f} + T$ and with formula 3 at $t_{p,f}$. Dashed lines are only for better visualization.

Figure 4 shows the evolution of the liquid stratification. At $t_{p,0}$, there is no stratification. After pressurization, at $t_{p,f}$, the maximal gradient in the temperature stratification appeared and the thermal boundary layer is from H_l to T2. Afterwards, at $t_{p,f} + T$, the thickness of the thermal boundary layer is increased below T2 and the temperature gradient is less sharp as the pressure has decreased. For better presentation in figure 4, only the temperature sensors T1, T2, T3 and the saturation temperature are depicted. The sensor T8 has the same temperature as T1 over all analyzed time steps. The temperature at the free surface (H_l, dash-dotted line) is assumed the saturation temperature of the relating tank pressure and is calculated using the NIST database.[11] An approach in order to predict the evolution of the thermal stratification over time is the approximation of transient heat transfer in a semi-infinite body with constant initial temperature, according to Becker.[12] For this experiment, the initial temperature is the liquid temperature T_l and the boundary condition is that the surface temperature is suddenly changed and maintained at the new saturation temperature $T = T_{sat}$. Equation (1) is used for the prediction of the theoretical liquid temperature distribution at $t_{p,f}$ and $t_{p,f} + T$.

$$T - T_l = (T_{sat} - T_l)\,\mathrm{erfc}\left[\frac{H_l - z}{2\sqrt{D_t\, t}}\right] \tag{1}$$

The time t is zero at the beginning of the pressurization. Figure 4 shows the comparison of the experimental data and the theoretical thermal stratification for $t_{p,f}$ with the thermal diffusion coefficient D_t= 7.74e-8 m^2/s and for $t_{p,f} + T$ with D_t= 7.98e-8 m^2/s. The thermal diffusion coefficients refer to the saturation temperature of the respective tank pressures. The used theoretical approach fits very good for the time $t_{p,f}$ but underestimates the thickness of the thermal boundary layer for $t_{p,f} + T$ due to the fact that the heat input from the wall and the latent heat set free due to condensation are disregarded in the theory.

Figure 5 depicts the evolution of the thermal stratification in the tank ullage during the experiment from the free surface (H_l, the dash-dotted line) up to the inner side of the lid (T_{sat}, T4 to T7, T14 and T13). The saturation temperature at free surface is calculated using the NIST database.[11] At $t_{p,0}$, the temperature increases linearly between the saturation temperature at the free surface and the lid temperature. At $t_{p,f}$, the temperature sensor T14, next to the diffuser has the highest temperature and dominates the curve of the stratification. That strong thermal gradient decreases due to convection and conduction in the ullage and after relaxation, the linear temperature gradient reappears. At $t_{p,f} + T$, the upmost layer of the ullage is still heated up from the warm pressurant gas and defines the gradient of the thermal stratification which has below T14 again a nearly linear distribution to the free surface temperature. Also for the ullage stratification, theoretical approaches were chosen in order to predict the stratification evolution. For the stratification at $t_{p,0}$ and $t_{p,f} + T$, the theoretical approach is the steady-state heat conduction in a flat plate, according to Polifke.[13] Therefore, the vapor temperatures are calculated by Equation (2), where H_v is the height of the vapor phase (comp. figure 2).

$$T = T_{sat} + (T - T_{sat})\frac{z - H_l}{H_v} \tag{2}$$

As thermal boundary conditions, the saturation temperature and temperature sensor T14 are used. T14 is applied due to the fact that it has a larger influence on the stratification profile than the lid temperature. As this approach describes only linear temperature profiles it can be used for the prediction of the stratification at $t_{p,0}$ and $t_{p,f} + T$.

For the stratification profile after pressurization at $t_{p,f}$, the following formula for steady-state heat conduction in a cylinder is applied, according to Polifke.[13]

$$T = T_{sat} + (T14 - T_{sat})\frac{\ln(z/H_l)}{\ln((H_v + H_l)/H_l)} \tag{3}$$

Figure 5 compares the evolution of the stratification of the experiment with the theoretical approach. For all three time steps, the theory fits quite good to the experimental data. The theoretical stratification for $t_{p,f}$ shows the biggest discrepancy to the experimental stratification at sensor T7. One reason for that might be that the forced convection, caused by the diffuser flow, swirls up vapor from a lower, colder section to the sensor.

The presented theoretical approaches describe adequately the evolution of stratification for all performed experiments. The only issue for the prediction of the ullage stratification is that the vapor temperature at the diffuser has to be used as boundary condition, which might not always be available.

3. Required Pressurant Gas Mass

The objective of this study was to investigate the required pressurant gas mass for a defined tank pressure raise. Therefore, the pressurant gas inlet temperature is measured during the experiments and the pressurant gas mass flow is kept constant at 40 L/min for air at 101.3 kPa and 273.15 K which results in a maximum mass flow of 8.324 e-4 kg/s for GN2 and 1.624 e-4 kg/s for GHe. The required pressurant gas mass is then calculated by the mass flow multiplied with the needed pressurization time. Figure 6 shows the required pressurant gas masses for all performed experiments over the pressurant gas temperature. The pressurant gas temperature, used for this figure is the inflow temperature T15. It can be nicely seen in figure 6, that for the GN2 experiments (green markers) the lowest pressurant gas temperature of 144 K required the most pressurant gas mass. The pressurant gas temperature of 263 K required only little more gas mass than with 352 K for the GN2 as well as for the GHe experiments.

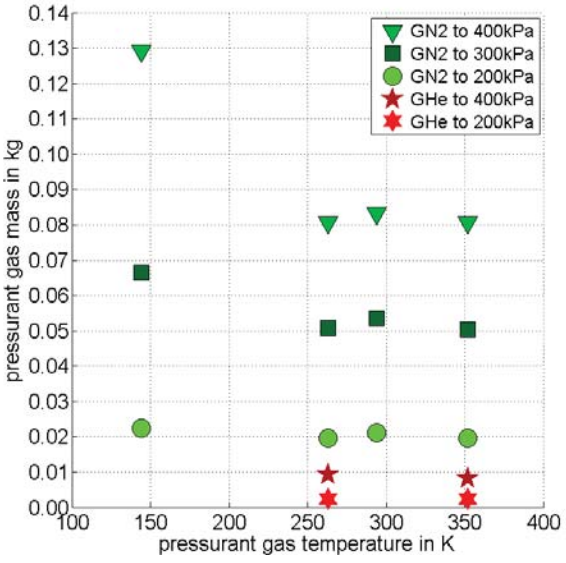

Figure 6. Required pressurant gas mass for all experiments over pressurant gas temperature T15

The interesting fact is that for the GN2 experiments the inlet temperature of 294 K needed more pressurant gas mass than for the 263 K inlet temperature. This is due to the fact that for all experiments, the pipe between the dewar inlet valve and the diffuser had to be warmed up or cooled down to the pressurant gas inlet temperature. As the lid and therewith also the inlet pipe had an initial average temperature of 278 K, the inlet pipe had to be cooled down only a few degrees to adapt to the pressurant gas temperature of 263 K. Therefore, less pressurant gas mass is required than expected.
Figure 7 depicts the tank pressure evolution for all four performed experiments pressurized with GN2 up to 300 kPa. The experiments with the lowest pressurant gas temperature of 144 K took the longest to reach 300 kPa which explains that it needed the most pressurant gas mass of all GN2 experiments. It can be seen that the GN2_300kPa@263K experiment had almost the identical slope for the pressure increase as did the GN2_300kPa@352K experiment. This confirms that the experiment with 263 K gas temperature required only little more gas mass than with 352 K. All four experiments nicely depict the pressure drop after the end of the pressurization to approximately 250 kPa.

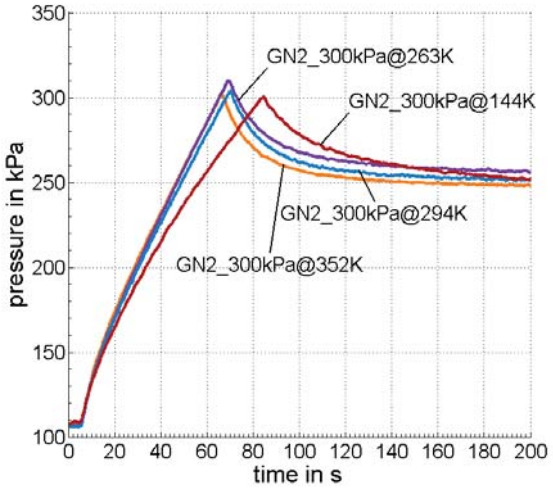

Figure 7. Tank pressure evolution for the GN2 pressurization up to 300 kPa with the four different pressurant gas temperatures

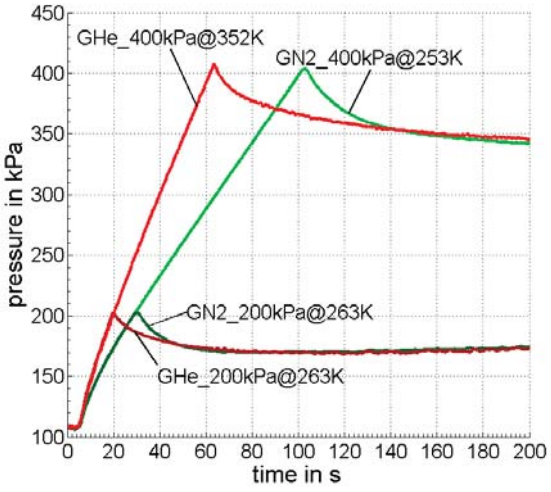

Figure 8. Comparison tank pressure evolution for the GN2 and GHe pressurization up to 200 kPa resp. 400 kPa with pressurant gas temperatures of 263 K and 352 K.

Figure 8 compares the pressure curve of two GHe experiments with the referring GN2 experiments. It can be see that for both GHe pressurizations, the pressure increases steeper than for the GN2 pressurizations. The faster pressurization happens on the one hand because helium is an inert gas and can not condense during pressurization process and on the other hand because it has a much lower density than nitrogen, which means that less GHe is needed to fill the tank ullage. Moreover, figure 6 shows that all helium pressurizations (red markers) require much less pressurant gas than the corresponding GN2 experiments, since helium has a very low molecular weight, which results in general in a low fluid mass.

III. System Study

The department of Space Launcher Systems Analysis (SART) at the DLR Institute of Space Systems applies the in-house program PMP (Propellant Management Program) for the preliminary design of propellant management systems for launcher and launcher related objects. Based on the experimental results, presented in chapter II, a system study of a cryogenic upper stage was performed. PMP was used to calculate the fluid masses and to estimate the propellant management system mass. The objective of this design study was to assess a similar range of pressurant gas inlet temperatures as in the experiments with regard to the influence on the mass of the entire upper stage. A description of the design of the investigated stage and the results derived from the PMP calculations are presented hereafter.

A. TSTO Launcher Design

At SART, a novel launcher concept is studied with the intention to base the design on technologies already existing in Europe and to benefit from synergies of different European launcher programs. This technological choice could lead to a reduction of development and production costs as well as an increase of the quality of production due to higher production quantities of some components, already used on other launchers. This concept is a Two-Stage To Orbit (TSTO) launch vehicle with a solid rocket motor for the first stage, which is using the same technologies as the P80 FW of Vega, as well as a cryogenic upper stage propelled by the 180 kN Vinci expander cycle engine with its deployable nozzle, intended to be applied for the next European heavy lift launcher. The goal of this TSTO launcher is to fill the performance gap between Vega and Soyuz by being used, for example, for Galileo satellite replacement single launch missions or, if needed, even to replace Soyuz for launch from Kourou by adding strap-on boosters.

Since 2011, this concept has been studied at SART. Various concepts of the TSTO launcher first and second stage were evaluated.[14] Based on that, a subsequent study on the variation of the solid rocket motors was performed in early 2012.[15] The system study presented in this paper is premised on this work and has the objective to focus on the propellant management system of the cryogenic upper stage in order to decrease the mass of the upper stage.

The selected reference trajectory, already applied for the foregoing studies, is the GTO (geostationary transfer orbit at 250 km x 35943 km, 5.4°) and corresponds to launches from Kourou in French Guiana. The applied TSTO launcher configuration is one of the most promising designs: the P170 type 3 + H26 + (2+2) P23 configuration. It has a payload performance into GTO of over 3 tons. Two pairs of P23 strap-on boosters, from which one pair is ignited with delay, assist the 170 tons solid rocket motor of the first stage. A high maximum acceleration of 4.9 g is reached during ascent. Afterwards the cryogenic upper stage, called H26 (see figure 9) is used to reach the preset orbit.

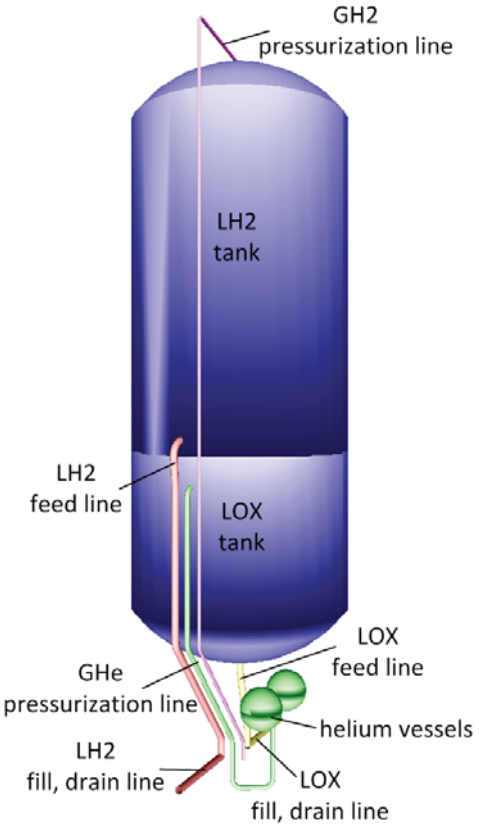

Figure 9. Design of the H26 upper stage with feed, fill and drain lines, pressurization lines and helium vessels

B. PMP Results for the H26 Upper Stage

For the preliminary design of the H26 upper stage, PMP was used for the calculation of the tank length, the fluid masses and estimation of the propellant management system mass. The results of the calculations are presented hereafter.

1. Fluid Masses

For the H26 upper stage, the high performances Vinci engine was chosen, as it is the most powerful upper stage engine available in Europe (propellants LOX/LH2, $I_{sp,vac}$= 464s, propellant mass flow 39.5 kg/s, mixture ratio 5.8). The engine burns for 658 s. For the propellant tanks, the common bulkhead architecture with a diameter of 3.5 m has been selected in the previous study. For the sizing of the propellant tanks, the following propellant masses were applied: The nominally used propulsive propellant mass is 26000 kg and the geometrical and thermal residuals are 149 kg. The propellant reserve mass is estimated at 448 kg. For the consumption of the Vinci engine during transient phases, which are the start and shut down phases, the chilldown maneuver, the thermal conditioning of the lines and the engine, as well as the lines priming, which is the initial filling of the feed lines with propellant, a total propellant mass of 250 kg is calculated. This results in a total propellant mass of 26847 kg.

The resulting total length of the common bulkhead propellant tanks is 9.9 m. The ullage volume of the LH2 tank is chosen so that the tank size can be kept constant over this study even if the hydrogen mass changes by the amount of GH2 required for the pressurization. The tank pressures were defined as 240 kPa for the LH2 tank and 220 kPa for the LOX tank. For this study, the tank pressure was kept constant over the whole burning time. It will be optimized in a later design loop together with the structural optimization of the upper stage.

The objective of this study was to optimize the required pressurant gas mass of the H26 upper stage based on the results presented in chapter II. One main outcome of the experiments was that for evaporated propellant as pressurant gas, the maximum applicable gas temperature is best for reducing the needed pressurant gas and that the application of helium is also very advantageous with regard to lowering the pressurant gas mass. Therefore, for H26 upper stage, gaseous hydrogen (GH2) was chosen for the pressurization of the LH2 tank. This GH2 will be tapped off the feed lines. For the LOX tank, gaseous helium was selected as pressurant gas, which has to be stored in one or more external tanks. In order to study whether a very high pressurant gas temperature is still advantageous when the total propellant management system is regarded, different pressurant gas temperatures in a reasonable temperature range from 100 K to 380 K were evaluated for H26 and the required pressurant gas masses were calculated with PMP. Figure 10 shows the results for the required GH2 and GHe pressurant gas masses over the different inlet temperatures. It can be seen that the required pressurant gas mass decreases for both gases with increased pressurant gas inlet temperature. For the GH2 pressurization, the required mass decreased about 18 kg between an inlet temperature of 100 K and 380 K. For GHe, the mass reduction was about 13 kg. These results correspond to the experimental results of chapter II. The reason why more GHe than GH2 is required for the H26 stage is because hydrogen has a liquid temperature of 20 K and oxygen about 90 K. That means that hydrogen evaporates faster than the oxygen under external heat flows and therewith already increases its tank pressure.

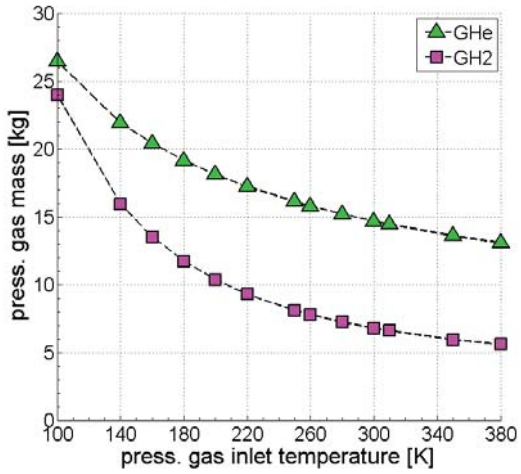

Figure 10. Required pressurant gas masses for GH2 and GHe at different pressurant gas inlet temperatures

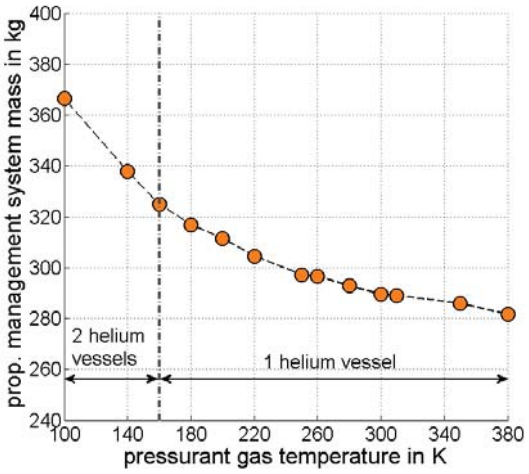

Figure 11. Propellant management system mass of H26 at different pressurant gas inlet temperatures

2. Propellant Management System Mass

In the next step, the influence of the different pressurant gas temperatures on the total propellant management system mass was evaluated. The total mass of the propellant management system was calculated with PMP and consists of the feed, fill and drain as well as pressurization line masses, the required pressurant gas masses as well as the helium vessel(s). Figure 9 depicts the H26 upper stage design, illustrating the propellant tanks with the LOX and LH2 feed, fill and drain lines (red and yellow) and GH2 and GHe pressurization lines (magenta and green) as well as the external helium tanks (green). The masses for the feed, fill and drain lines were computed for LOX as 43 kg and for LH2 as 66 kg, including the insulation mass. The mass of the pressurization lines was estimated as 48 kg for GH2 and 53 kg for GHe. For the helium

vessels, including fixation, the tank design from the Ariane 5 EPC and EPS program was applied. The vessel mass was scaled to the required helium volume for a helium storage temperature of 288 K and 40000 kPa. Figure 11 depicts the mass of the total propellant management system over the different pressurant gas inlet temperature, based on the results of the previous section. For the helium temperature from 100 K to 160 K, two external vessels were required for the H26 stage, which additionally increase the stage's mass. For the pressurant gas temperatures of 180 to 380 K, only one vessel was required. The required vessel mass decreased with the decreasing amount of helium needed. The mass saving by using a pressurant gas inlet temperature for both fluids of 380 K instead of 100 K is 85 kg. Therewith follows that also for the total propellant management system, an increased pressurant gas inlet temperature decreases the system mass and is therewith advantageous for cryogenic upper stages.

IV. Conclusion

The objective of this paper was to analyze the influence of the pressurant gas temperature on the required pressurant gas mass in terms of lowering the launcher's mass. Therefore, ground experiments were performed in order to investigate the pressurization process with regard to the influence of the pressurant gas inlet temperature on the required pressurant gas mass. As pressurant gases, gaseous nitrogen and gaseous helium were analyzed at different inlet temperatures. The experimental set-up was described and the procedure for the experiments was presented. The evolution of the tank pressure and the temperatures in the liquid and vapor phase were investigated. One important effect was that after the end of the active-pressurization, a pressure drop occurred. The main reason is the condensation of the vapor phase. This pressure drop decreases over time and the tank pressure asymptotically approaches a final pressure as the condensation and evaporation reach an equilibrium. This experimental result leads to the awareness that for a constant tank pressure, continuous pressurization of the propellant tanks is essential.
In the next step, the history of the fluid stratification was evaluated at three characteristic times. Thereby, the flange of the dewar was identified as a major heat source, influencing the stratification in the vapor and liquid phase. For the liquid phase, a thermal boundary layer was established, with increasing thickness over time. For the vapor phase, the injected pressurant gas had major influence on the gradient of the thermal stratification. The thermal stratification of the liquid and the vapor phase was predicted with a theoretical approach and the accordance with the experimental data was very good.
Subsequently, the required pressurant gas was analyzed with regard to the used pressurant gas and pressurant gas temperature. An important result was that, especially for the gaseous nitrogen pressurization, an increased pressurant gas temperature accelerated the pressurization process and decreased therewith the required pressurant gas mass. One exception was the pressurant gas temperature near the initial temperature of the inlet pipe, which required lower pressurant gas mass than expected. This exposed that the heating respectively the cooling of the diffuser pipe also increases the pressurant gas need. In addition, the use of helium as pressurant gas is advantageous as it cannot condense and has a low molecular weight and density. These results led to the conclusion that the highest pressurant gas temperature need the lowest pressurant gas mass, on condition that the pressurization lines are already chilled down in advance.
Based on these experimental results, a system study for a small Two Stage to Orbit (TSTO) launch vehicle was performed. The objective was to evaluate the influence of the pressurant gas temperature on the whole propellant management system mass. Therefore, several pressurant gas temperatures were applied. Together with the calculated propellant mass and the masses of the lines, the optimal propellant management system mass for H26 was selected. The result of this system study was that, despite the application of helium as pressurant gas with the additionally needed gas vessels, the highest pressurant gas temperatures for both tanks resulted in a mass saving of 85 kg. This might not seem much compared to the total stage mass, but it should be remembered that every kilogram saved on an upper stage can directly be converted to additional payload performance. It is also a relevant mass reduction, which leads to the conclusion that, for the total propellant management system as well, the highest pressurant gas temperature leads to the lowest system mass.
Based on that outcome, the next step will be to investigate how the pressurant gases should be best heated up to their maximal possible temperature. One possibility is a heat exchanger (e.g. at the engine) and an optimal design of this device could be investigated in the next TSTO upper stage study. Constraints for the maximum applicable pressurant gas temperature are determined by component reliability issues of the pressurization system, the tank wall temperature limitations and the effort to miminize thermal residuals.

Acknowledgments

The authors acknowledge gratefully Peter Prengel, Frank Cicerior and Peter Friese for their effort in preparing and performing the experiments and Etienne Dumont for the contributions to the TSTO configurations.

References

[1]Ring, E., *Rocket Propellant and Pressurization Systems*, Prentice-Hall, 1964.

[2]Nein, M. E. and Thompson, J. F., "Experimental and analytical studies of cryogenic propellant tank pressurant requirements," 1966, NASA TN D-3177.

[3]Stochl, R. J., Masters, P. A., DeWitt, R. L., and Maloy, J. E., "Gaseous-hydrogen requirements for the discharge of liquid hydrogen from a 3.96-meter- (13-ft-) diameter spherical tank," 1969, NASA TN D-5387.

[4]Stochl, R. J., Masters, P. A., DeWitt, R. L., and Maloy, J. E., "Gaseous-hydrogen requirements for the discharge of liquid hydrogen from a 1.52-meter- (5-ft-) diameter spherical tank," 1969, NASA TN D-5336.

[5]Stochl, R. J., Maloy, J. E., Masters, P. A., and DeWitt, R. L., "Gaseous-helium requirements for the discharge of liquid hydrogen from a 1.52-meter- (5-ft-) diameter spherical tank," 1970, NASA TN D-5621.

[6]Stochl, R. J., Maloy, J. E., Masters, P. A., and DeWitt, R. L., "Gaseous-helium requirements for the discharge of liquid hydrogen from a 3.96-meter- (13-ft-) diameter spherical tank," 1970, NASA TN D-7019.

[7]van Dresar, N. T. and Stochl, R. J., "Pressurization and expulsion of cryogenic liquids: Generic requirements for a low-gravity experiment," 1991, NASA Technical Memorandum 104417.

[8]van Dresar, N. T. and Stochl, R. J., "Pressurization and Expulsion of a Flightweight Liquid Hydrogen Tank," 1993, AIAA-93-1966.

[9]Himeno, T., Konno, A., Tsuboi, M., and Fukuzoe, M., "Numerical Investigation of Liquid Behavior in the Propellant Tank of H-IIA," 2002, AIAA-2002-3987.

[10]Baehr, H. D. and Kabelac, S., *Thermodynamik: Grundlagen und technische Anwendungen*, Springer, 2009.

[11]Lemmon, E. W., Huber, M. L., and McLinden, M. O., *NIST Standard Reference Database 23: Reference Fluid Thermodynamic and Transport Properties-REFPROP*, National Institute of Standards and Technology, Standard Reference Data Program, 2010.

[12]Becker, M., *Heat Transfer: A Modern Approach*, Springer US, 1986.

[13]Polifke, W. and Kopitz, J., *Wärmeübertragung. Grundlagen, analytische und numerische Methoden*, Pearson Studium, 2005.

[14]Dumont, E., Ludwig, C., Kopp, A., and Sippel, M., "Advanced TSTO Launch vehicles," *4th European Conference for Aerospace Sciences, Saint Petersburg, Russia. EUCASS 2011-253*, 2011.

[15]Dumont, E., "Variations of Solid Rocket Motor Preliminary Design for Small TSTO launcher," *Space Propulsion 2012, Bordeaux, France. ID 2394102*, 2012.